

# Light backscattering from large clusters of densely packed irregular particles

YEVGEN GRYNKO<sup>A,\*</sup>, YURIY SHKURATOV<sup>B</sup>, JENS FÖRSTNER<sup>A</sup>

<sup>A</sup>*Department of Theoretical Electrical Engineering, Paderborn University, Warburger Str. 100, 33102 Paderborn, Germany*

<sup>B</sup>*Institute of Astronomy of Kharkiv National University, Sumska Str. 35, 61022 Kharkiv, Ukraine*

\*Corresponding author: [yevgen.grynko@upb.de](mailto:yevgen.grynko@upb.de)

*Keywords:* radiative transfer, disordered media, polarization

## Abstract

We numerically simulate multiple light scattering in discrete disordered media represented by large clusters of irregular non-absorbing particles. The packing density of clusters is 0.5. With such conditions diffuse scattering is significantly reduced and light transport follows propagation channels that are determined by the particle size and topology of the medium. This kind of localization produces coherent backscattering intensity surge and enhanced negative polarization branch if compared to lower density samples.

## 1. Introduction

Optical properties of discrete disordered media are studied in various fields like remote sensing, photonics and biology. For instance, optimization of random lasers [1], beam shaping and focusing in random media [2], remote sensing applications in geophysics and planetary science [3, 4] require theoretical modeling of light scattering in dense many-particle structures. Various transport phenomena like weak and strong (Anderson) localization of light [5, 6] are predicted and observed for dense media with high degrees of disorder. This regards not only classical electromagnetics but also quantum optical systems [7, 8]. In classical optics such properties can be utilized for controlled transmission and backscattering from granular slabs (e.g., [9, 10]) as well as retrieval of the information about physical properties of a medium from optical measurements, i.e. solving the inverse problem [4].

We are interested in numerical simulations of light backscattering from powder-like surfaces and interpretation of the photopolarimetric data obtained from laboratory measurements and optical observations of the remote objects like surfaces of the Earth and the Solar System bodies. Such surfaces are formed by randomly shaped particles with different sizes and mineral materials that are densely packed up to a packing density value of  $\rho = 0.5$ . Optical opposition phenomena like intensity surge (IS), i.e. nonlinear enhancement of intensity, and negative polarization (NP) (e.g., [11-13]) of light scattered at large scattering angles are often observed for this kind of targets. Their parameters depend on the physical properties of the scatterers and the structure of the upper surface layer. Hence, such dependences can be utilized in the data retrieval.

The backscattering response from particulate surfaces is a combination of single scattering from individual particles and multiple coherent and incoherent scattering in the bulk medium. Isolated irregular

particles are known to produce backscattering intensity enhancement and a strong NP branch (e.g., [14, 15]). At the same time coherent multiple scattering is also a strong factor that presumably stands behind both phenomena [16-21]. However, the specific role of single and multiple scattering in a dense medium and their relative contributions to backscattering remain unclear and require further theoretical studies. There are also a few more specific questions that should be addressed. In particular, it is important to have an estimate of the mean transport length of light in a non-absorbing or moderately absorbing dense medium consisting of irregular particles slightly larger than the wavelength. This can give an idea of how thick the surface layer is that forms backscattering response carrying information about its physical properties. Also, one has to know how large a finite sample should be to be a representative scattering volume which is a basic element in the radiative transfer models. This includes also the characteristic spatial scale of multiple scattering effects that contribute to IS and NP. Direct time-domain simulations with a realistic model can also display the exact pattern of the near field interaction of irregular particles larger than the wavelength if they are placed in close vicinity of each other. After all, a technical question is open: how large samples with random irregular particles can be handled in a systematic study with available high-performance computing (HPC) resources and a versatile Maxwell solver.

The solution of the problem requires numerical methods that allow description of arbitrary geometries of individual scatterers and their dense placement. Due to the general complexity of the task simulations avoiding approximations have not been done so far for such structures. We note that random irregular constituent shapes should be taken into consideration as scatterers with perfect geometries cannot be representative due to their peculiar optical properties. The geometry of individual scatterers also determines the medium topology at dense packing which also should be taken into account. Additionally, one should consider systems much larger than the wavelength of the incident light and with large enough number particles to adequately simulate collective scattering effects. On the other hand, dense packing implies that the distances between constituents are much smaller than the wavelength. Thus, the listed conditions make the problem multi-scale which requires HPC hardware and numerical methods that allow efficient parallelization.

Simulations of light scattering in multi-particle systems and very large sizes and arbitrary shapes of constituent particles are possible in the geometric optics (GO) approximation [22-30]. An obvious limitation of the GO models is that wave optics effects are usually not taken into account and, therefore, backscattering cannot be modeled correctly.

A recent development of a hybrid approach [31] in which ray tracing in a dense medium is supplied with accounting for coherent backscattering enhancement, allowed numerical simulation of multiple scattering in a very large sample and comparison with experimental laboratory of an agglomerate made of micrometer-scale silica spheres [32]. However, in that work backscattering region has been omitted and the performance of the model is not known in this case.

Successful wave-optics simulations of light scattering by very large samples based on the superposition T-matrix method and parallel CPU/GPU implementations have been reported recently (e.g., [33-35]). However, such simulations are possible for dense systems of spherical particles only. The T-Matrix method formulation uses vector spherical harmonics for decomposition of the field at distances larger than the radius of the smallest sphere circumscribing a particle. Therefore, it becomes invalid in a multi-particle structure with non-spherical particles placed in the near field of each other closer than the sphere radii.

In a recent work [36] a promising method called the global polarizability matrix has been introduced. In its formulation a circumscribing sphere can be replaced by a surface of arbitrary shape, e.g., matching the shape of an individual particle, thus, allowing dense packing and correct accounting for the near-field interaction of closely placed groups of particles. As an example, a light scattering problem for a cluster of identical rods is considered in the paper. For practical applications the performance of the method for structures consisting of hundreds/thousands of random particles should be tested.

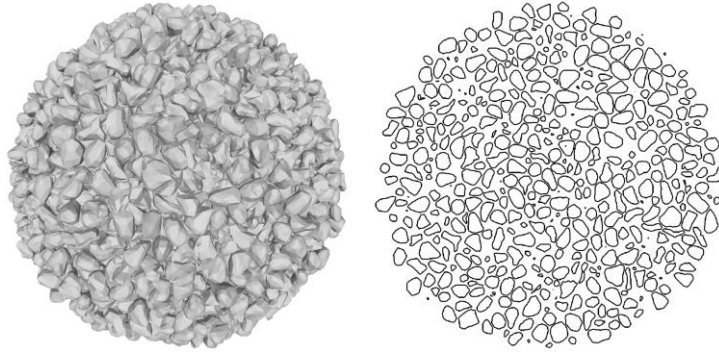


Figure 1: Spherical cluster with  $N = 5000$  particles and packing density  $\rho = 0.5$  and its cross-section.

---

## 2. Model description

Here we apply a model that represents realistic structure of powder samples. We consider dense systems of random irregular particles with sizes comparable to or larger than the wavelength of the incident light. A 3D electromagnetic problem is solved numerically avoiding approximations and using the Discontinuous Galerkin Time Domain (DGTD) method [37]. It is based on unstructured meshing and its numerical scheme can be parallelized with high efficiency.

The simplest target geometry that allows simulation of light scattering in the entire range of scattering angles is a sphere. Therefore, we consider spherical clusters of particles. Model cluster preparation includes generation of constituent shapes and their packing with large enough packing density. As in our previous works on light scattering by isolated particles, we use Gaussian Random Field (GRF) shapes [14, 15, 38-39]. Having a large pre-generated set of particle samples represented by triangular facets we can apply the particle packing routine.

Basic random uniform distribution of non-overlapping irregular shapes allows densities up to  $\rho \approx 0.1$  [22,28]. Generation of model media with  $\rho > 0.1$  is, however, a challenging task: one has to apply special algorithms that minimize free space between particles accounting for their irregular shapes. In Ref. [23] we used simple Boolean summation of a few pre-generated media samples with  $\rho = 0.1$  reaching the total density of  $\rho = 0.3$ . In Refs. [28, 29] we applied isometric inflation with Monte Carlo rotation of particles. The maximum packing density achieved with such an approach was  $\rho \approx 0.4$ .

Here we apply the Bullet physics engine [40] which simulates dynamics and interaction of multiple geometrical objects in time domain. In this framework we use a point gravity source positioned in the center of the sparsely and uniformly distributed initial set of particles. Adjusting their friction and the parameter of minimal distance between neighbors one can simulate evolution of such a set into a spherical cluster with densities up to  $\rho \approx 0.55$ . Fig. 1 shows an example of such a cluster and its cross-section. The sample consists of  $N = 5000$  particles packed with  $\rho = 0.5$ .

We consider three cases of clusters with size parameters  $kR = 50, 100$  and  $150$  ( $k$  is the wave number and  $R$  is the particle radius). The size of constituents is taken  $kR_c = 10$  which corresponds to the numbers of particles of  $N = 200, 1600$  and  $5000$  for the corresponding cluster sizes. The packing density is  $\rho = 0.5$  in all cases. For the size  $kR = 100$  we also study the role of packing density and consider two separate cases with relatively sparse packing of  $\rho = 0.16$  and uniform and non-uniform distributions of constituent particles.

The material is non-absorbing in all cases and the complex refractive index is  $m = 1.5 + 0i$ .

After a sample of a cluster is generated it is taken as an input in a tetrahedral mesh generator. Discretization of space in a structure with very close placement of constituents requires high spatial resolution in the corresponding regions. Unstructured meshing with local mesh refinement becomes very helpful here. An important factor, that makes an impact on the total simulation time, is the reduction of the time step in the explicit time integration of Maxwell's equations in the DGTD numerical scheme due to the presence of small elements. Thus, for the numerical packing we choose a small but non-zero parameter for the minimum distance between particles keeping it much smaller than the wavelength and maintaining large packing density values and an acceptable time step value.

We consider plane wave as an illumination source and use total field/scattered field technique to simulate propagation of a plane wave in a finite domain. Unpolarized light source is simulated by means of two simulation runs with linearly polarized illumination with perpendicular polarizations. Perfectly matching layer boundary conditions are used to model light scattering in open space.

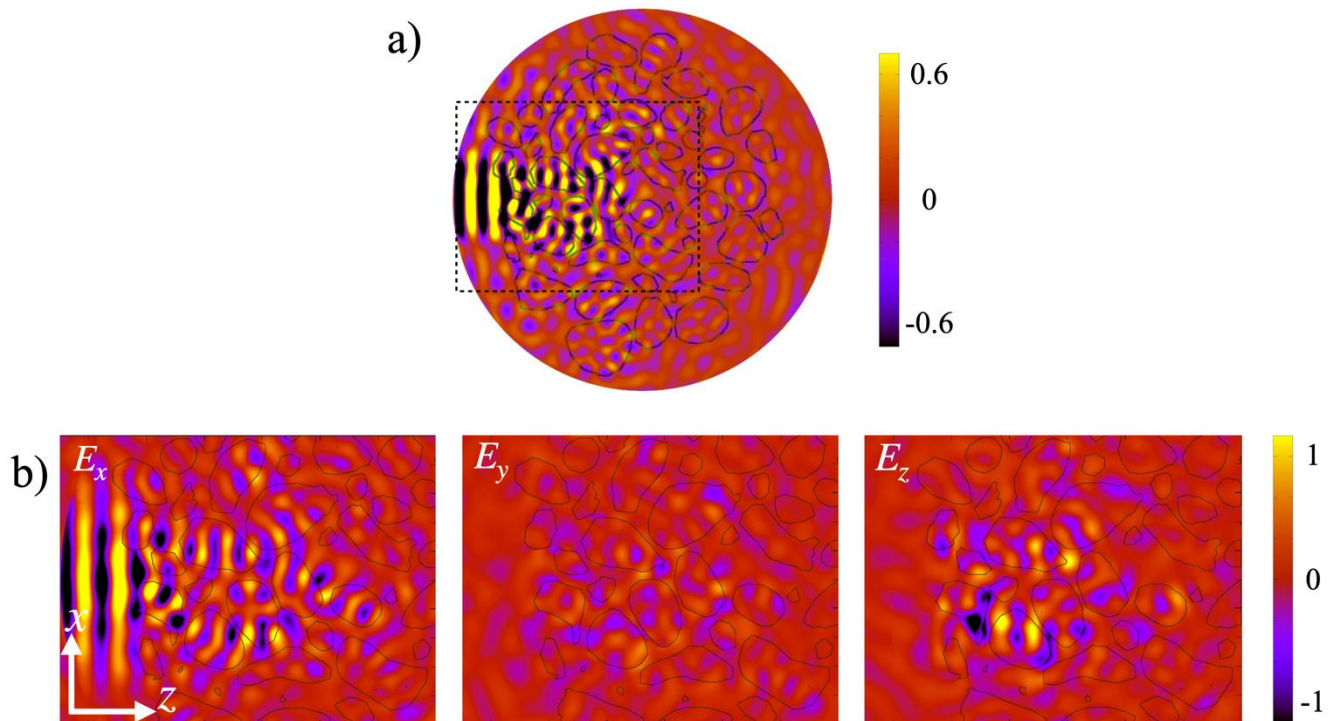


Figure 2: Snapshot of the electric field amplitude component  $E_x$  propagating in  $Z$  direction in a cluster with 200 particles (a) and an enlarged fragment showing distributions of the three components of the electric field (b). The incident beam is  $E_x$ -polarized.

The computed and measured scattered near field around a cluster is transformed to the far field [39] and the scattering matrix elements are obtained as functions of the scattering angle. The curves are averaged for each cluster size over 10 samples with 6 orientations per sample and over azimuth angle.

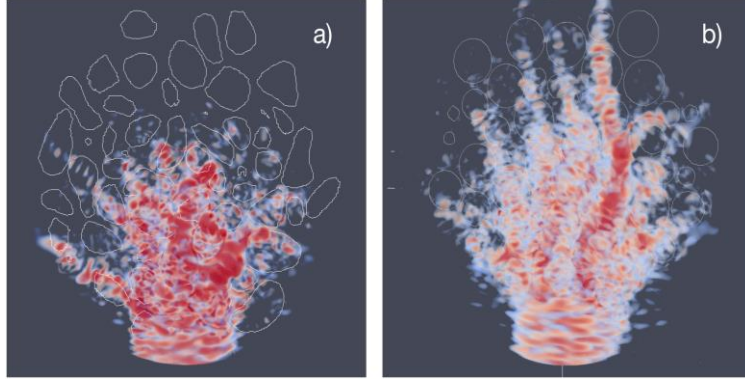


Figure 3: Distribution of the logarithm of intensity ( $\log(|E|^2)$ ) of the near field in dense clusters of 200 irregular (a) and spherical (b) particles.

### 3. Results and discussion

At first, we analyze the light transport pattern, i.e. near field distribution as a light beam propagates through a cluster. This may give us better understanding of the near-field interaction between close neighbors and its role in the formation of the far-field scattering quantities. For this purpose, we simulate illumination with a focused beam in order to localize the entrance spot on the surface of a cluster. The cross-section of the beam is smaller than the cluster size and it illuminates only a few particles on the surface. In Fig. 2a we show a 2D snapshot of the  $E_x$  component of the resulting internal electric field distribution. The incident beam is  $E_x$ -polarized and propagates in  $Z$  direction. The cluster has the size of  $kR = 50$  and consists of  $N = 200$  particles. This is a typical pattern that is different for different samples but its structure always remains the same. Here, a high packing density of particles becomes a key factor that significantly changes the pattern of light transport in comparison to multiple scattering in sparse media.

After transmission by particles in the very upper layer light follows chains of particles in the depth which form propagation channels. This behavior is polarization independent, i.e. waves with different polarizations follow the same propagation paths. Near field interaction includes focusing on the neighbor particle after transmission and whispering gallery wave coupling between the surfaces of the neighbors. Such threads can also split, if two particles are hit on the way, and form random fractal geometry. One can see also in Fig. 2b that the  $E_z$  component of the electric field gets enhanced on the way with hotspots located in the regions of the near field interaction between close particles. This indicates an important role of the radial component in the propagation. It quickly decays with distance as  $\sim 1/r^3$  but becomes influent at dense packing. In general, such mechanism results in a percolation-like transport that is determined by the fractal topology of the medium.

For better illustration we present the result of the same simulation in 3D view. In Fig. 3a we visualize the logarithm of intensity in frequency-domain, i.e.  $\log(|E|^2)$ , distributed in the cluster in the form of the volume color map. The colored structure spans over 90% of the total near-field energy which means high localization of light in the propagation channels and little diffuse unpolarized scattering. Measuring fractal

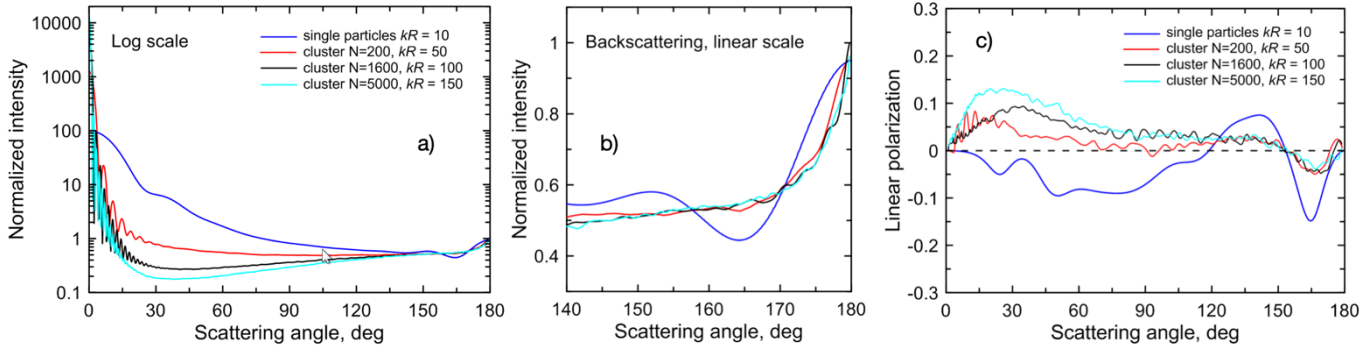


Figure 4: Computed scattering angle dependencies of intensity in logarithmic scale (a), linear scale near backscattering (b) and the degree of linear polarization (c) for single GRF particles with size parameter  $kR_c = 10$  and clusters of GRF particles with  $kR = 50, 100$  and  $150$  and  $\rho = 0.5$ .

dimension of such a computed energy distribution (e.g. [42]) one can characterize the complexity of a disordered medium which is an important geometric property in addition to the parameter of packing density. We note also, that the scattering matrix elements that are measured in the far field may also contain this kind of complexity information which can be potentially retrieved through photopolarimetric measurements.

We also calculated, for comparison, a similar energy distribution for a cluster consisting of 200 spherical particles with the same size and material packed with  $\rho = 0.5$ . Fig. 3b demonstrates how different the field pattern can be if the constituents have perfect spherical shapes. A medium of densely packed spheres has lower degree of disorder than that of irregular particles. As a result, such a topology forms more efficient wave guiding chains of particles.

With this finding we can refer to the so-called one-dimensional models of spectral albedo of powders [43,44]. In these models light propagation is approximated by multiple reflections and transmissions in a sequence of slabs with thicknesses equal to the average size of particles. In fact, this approximation is consistent with our result. Single propagation channels can be considered as 1D paths. High localization of light in the channels can explain why such a simple approximation can be valid, to some extent, in the wave optics regime.

In general, we see that light transport in a densely packed system of particles can be characterized as a percolation-like process rather than multiple scattering from particle to particle, or, from elementary volume to elementary volume, as it is usually described with conventional radiative transfer theory [45, 46]. We note, that in the case of the GRF cluster the characteristic transport length is smaller than the cluster size ( $kR = 50$ ). It can be even smaller at non-zero absorption. Accounting for the gradient of intensity at this scale and the complexity of the field distribution, that quickly changes with distance, the elementary volume approach cannot be valid in such conditions.

In Fig. 4 we compare the computed far-field scattering angle functions of intensity and polarization for three cluster sizes. We add also a “single-scattering” curve calculated for an ensemble of isolated GRF particles with  $kR_c = 10$ . Generally, the samples become less transparent with increasing size. At backscattering we observe an IS that is apparently caused by coherent propagation. Obviously, this is a property of the structure of clusters and not the size as in the case of

solid compact particles [13]. The curves in this angular range do not depend on the cluster size if it is large enough with respect to the wavelength and the size of constituents. In other words, angular dependency of intensity of scattered light should converge to the case of a semi-infinite medium with increasing cluster size and this convergence starts in the backscattering region.

The broad IS is a characteristic feature of single particles [14]. In principle, it may also contribute the total IS from a cluster making it less sharp. We note, that 1D coherent transport in the propagation channels, discussed above, may also contribute in the transport of energy in the backward direction.

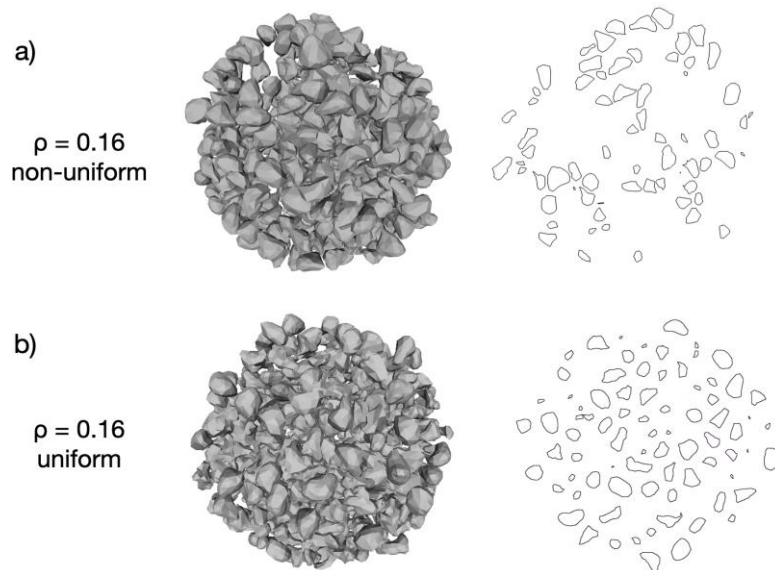


Figure 5: Two topologically distinct clusters with the same packing densities  $\rho = 0.16$ .

The linear polarization of forward scattering (small scattering angles) shows the effect of cluster edges where the curves are mostly formed by the positively polarized component reflected from external surfaces of particles in the upper layer of the cluster. This is in agreement with laboratory polarimetric measurements of powders at grazing angles of incidence [46] and also with our previous GO modeling [26]. The NP branch at large scattering angles is significantly reduced with respect to that of isolated particles. However, the inversion angle remains the same for all cluster sizes. This fact may indicate that NP is a result of contribution of single scattering from particles in the upper layer that is partially depolarized by the multiple scattering component. Although there is a large difference for clusters with different sizes at smaller angles, the curves near backscattering are quite close to each other. This suggests that the structure of clusters, which is the same in all cases, plays major role in the formation of the polarization angular dependence in this region.

For more insight into the role of topology and packing density we consider two cases of relatively sparse media with the same  $\rho$  but different particle connectivity patterns. First, we take the same set of cluster samples with  $kR = 100$  and remove  $2/3$  of all particles from each sample making a sparse structure with non-uniform distribution of constituents with  $\rho = 0.16$  and  $N = 530$  (Fig. 5a). Such clusters contain large voids and small agglomerates of a few particles. In the second case we generate

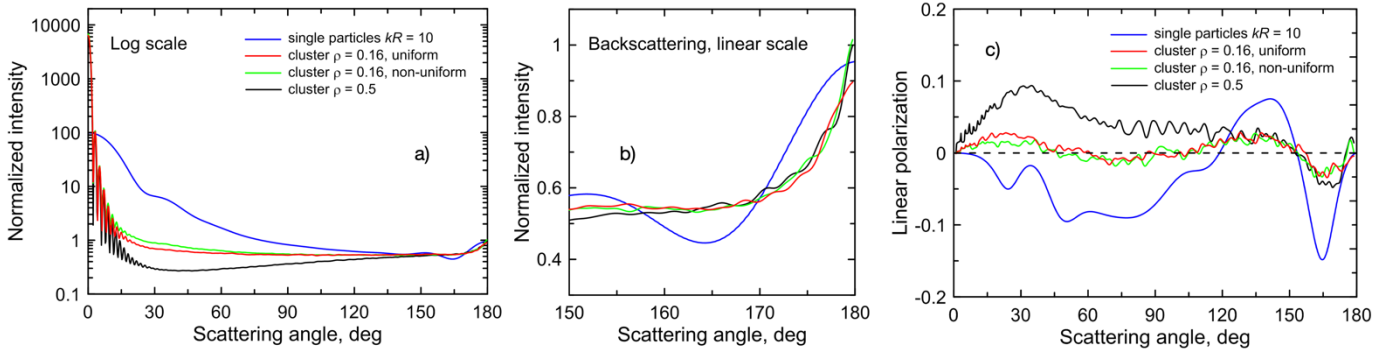


Figure 6: Computed scattering angle dependencies of intensity in logarithmic scale (a), linear scale near backscattering (b) and the degree of linear polarization (c) for single GRF particles with size parameter  $kR_c = 10$  and clusters of GRF particles with  $kR = 100$ :  $\rho = 0.16$ , uniformly distributed,  $\rho = 0.16$ , non-uniformly distributed and  $\rho = 0.5$ .

a new set of samples with simple uniform distribution and the same number of constituents, so that the packing density also remains the same (Fig. 5b).

In Fig. 6 we compare the IS and linear polarization curves for dense and sparse clusters. Interestingly, sparse clusters with non-uniform distribution of particles appear to be efficient enough for the coherent backscattering enhancement and are able to produce a sharp IS. This can be explained by the role of small agglomerates of particles which also characterizes the spatial scale of the collective coherent effects that form the IS.

If particles are sparsely and uniformly distributed in space, near-field interaction is obviously reduced revealing backscattering properties of single particles. The IS becomes different in this case and is somewhat similar to the single-scattering one. We note, that clusters with the same packing densities but topologically distinct produce different backscattering intensity response. Real granular surfaces may have quite sparse structure of the upper layer having packing density values as low as  $\rho = 0.1 - 0.3$  yet produce coherent backscattering IS. Therefore, sparse model media in correct simulations should not be uniform distributions of constituents but rather structures with small-agglomerate connectivity and large voids.

The difference in linear polarization between dense and sparse clusters is in good qualitative agreement with laboratory experiments with compressed low-absorption (high albedo) powder samples [19, 47, 48]. The results of laboratory measurements showed that compression of powder samples significantly increases negative and positive polarization features keeping the same inversion angle. This is also the case in our simulations and can be explained by light localization and, correspondingly, reduction of diffuse scattering. If there are large enough ( $\sim 10$  wavelengths in the non-uniform case) voids in a cluster, or the distances between constituents are large compared to the wavelength multiple scattering is still present but the scattered field turns into a diffuse background.

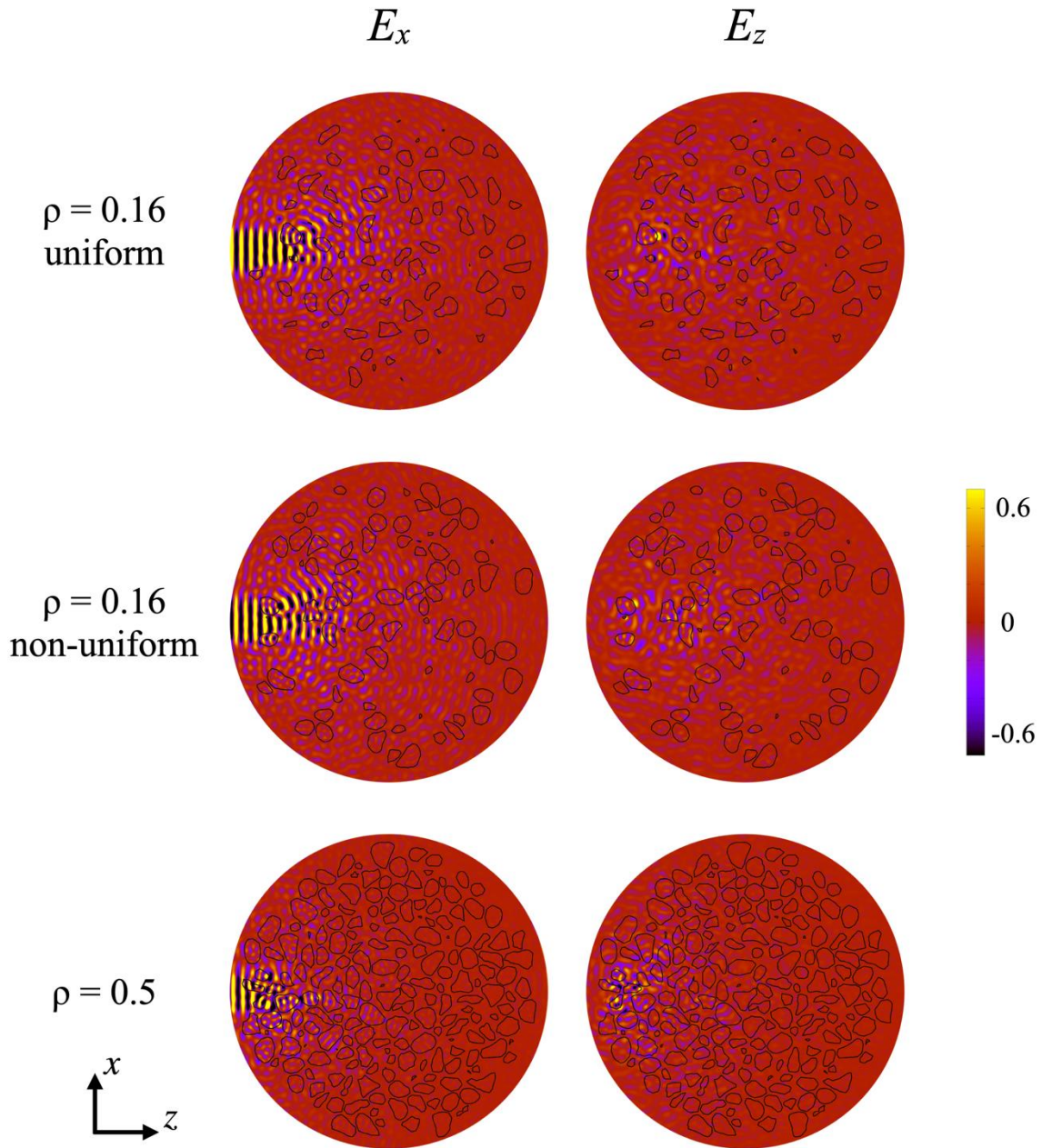


Figure 7: Steady state distributions of the electric field components  $E_x$  and  $E_z$  in sparse ( $\rho = 0.16$ ) and dense ( $\rho = 0.5$ ) clusters with size  $kR = 100$  illuminated by a focused beam.

This component is unpolarized to a high degree and suppresses strong polarization features of individual particles. As a result, we see similar but reduced positive and negative polarization features for clusters if compared to those for single particles. At  $\rho = 0.5$  light transport becomes localized, there is little space for energy to diffuse out of the localization regions and to produce the unpolarized component. Therefore, we see enhanced NP at backscattering and positive polarization of light reflected from the upper layer at smaller angles.

The above reasoning is supported by the analysis of the internal field distributions in the clusters with different structures. In Fig. 7 we show steady state snapshots of the  $E_x$  and  $E_z$  electric field components for the sparse and the dense samples with  $kR = 100$  probed with a focused beam with the same width and intensity. At  $\rho = 0.16$  the means of light transport is free space as the mean free path length is larger than the wavelength. As a result, we obtain a broad field distribution with many particles involved in multiple scattering and spanning the larger part of the cluster considering the narrow incident beam. In addition, one can see that the  $E_z$  component cannot participate in the process as it attenuates within one wavelength distance. High packing density crucially changes the mechanism of light propagation. The incident field interacting with the cluster surface becomes confined in a small region spanning just a few particles and further propagation is possible only if a favorable chain of particles is accidentally formed in a sample. This also supports the assumption that small agglomerates of particles are responsible for the formation of the IS in the cases of sparse clusters with non-uniform particle distribution.

Interestingly, the polarization curves for both kinds of sparse structures almost coincide in the entire range of scattering angles. Small agglomerates present in the clusters with non-uniform distributions of particles play small role here and, in particular in the NP region.

The polarization inversion angle near  $150^\circ$  for dense and both kinds of sparse clusters coincide with that of isolated particles. We believe this is a strong argument for single scattering as the main contributor in the NP near backscattering.

#### 4. Conclusion

In conclusion, our simulations show the importance of using high packing densities and irregular constituent particles for modeling of light backscattering from powder samples. Light propagation in the considered models of dense disordered media is localized and becomes similar to a percolation-like transport that is determined by the topology of the medium. The negative polarization near backscattering apparently originates from single scattering by particles in the surface layer and can be enhanced at large packing densities due to the reduced contribution of the diffuse component of multiple scattering. Such localization results also in coherent backscattering peak that appears to be independent on the cluster size at sizes  $kR > 100$ .

**Acknowledgment.** The authors gratefully acknowledge the computing time granted by the Paderborn Center for Parallel Computing (PC<sup>2</sup>) and by the John von Neumann Institute for Computing (NIC) on the supercomputer JURECA at Jülich Supercomputing Centre (JSC).

## References

- [1] Wiersma DS. The physics and applications of random lasers. *Nature Physics* 2008; 4:359–367.
- [2] Jeong S, Lee Y, Choi W, Kang S, Hong JH, Park J, Lim Y, Park H, Choi W, Focusing of light energy inside a scattering medium by controlling the time-gated multiple light scattering, *Nature Photonics* 2018; 12:277–283.
- [3] Photopolarimetry in remote sensing, G. Videen, Ya. Yatskiv, M. Mishchenko, eds., NATO Science Series, Netherlands: Kluwer Academic Publishers, 2004.
- [4] Segev M, Silberberg Y, Christodoulides D, Anderson localization of light, *Nature Photonics* 2013; 7:197–204.
- [5] Aegerter CM, Maret G, Coherent backscattering and Anderson localization of light, *Progress in Optics*, Elsevier, Volume 52, 2009, 1-62.
- [6] Popoff SM, Aubry A, Lerosey, Fink M, Boccardi AC, Gigan S, Exploiting the Time-Reversal Operator for Adaptive Optics, Selective Focusing, and Scattering Pattern Analysis, *Physical Review Letters* 2011; 107:263901.
- [7] Labeyrie G, Coherent transport of light in cold atoms, *Modern Physics Letters* 2008; B 22: 73–99.
- [8] Kupriyanov DV, Sokolov IM, Havey MD, Mesoscopic coherence in light scattering from cold, optically dense and disordered atomic systems, *Physics Reports* 2017; 671:1-60.
- [9] Vellekoop IM, Feedback-based wavefront shaping, *Optics Express* 2015; 23:12189.
- [10] Polarimetry of Stars and Planetary Systems, Eds.: L. Kolokolova, J. Hough, A.-C. Levasseur-Regourd, Cambridge University Press 2015, 487 p.
- [11] Lyot B, Recherches sur la polarisation de la lumiere des planetes et de quelques substances terrestres, *Ann. Obs. Meudon* 1929; 8.
- [12] Shkuratov Y, Videen G, Kreslavsky M, Belskaya I, Kaydash V, Ovcharenko S, Omelchenko V, Opanasenko N, Zubko E, Scattering properties of planetary regoliths near opposition, in *Photopolarimetry in remote sensing 2004*; G. Videen, Ya. Yatskiv, M. Mishchenko, eds., NATO Science Series, Netherlands: Kluwer Academic Publishers, 191–208
- [13] Mishchenko M, Rosenbush V, Kiselev N, Lupishko D, Tishkovets T, Kaydash V, Belskaya I, Efimov Y, N. Shakhovskoy N, Polarimetric remote sensing of Solar System objects (*Akadempriodyka*, Kiev, 2010).
- [14] Grynko Y, Shkuratov Y, Foerstner J, Intensity surge and negative polarization of light from compact irregular particles, *Optics letters* 2018; 43:3562-3565.
- [15] Grynko Y, Zubko E, Foerstner J, Light scattering by random irregular particles of two classes of shape, *Optics letters* 2014; 39:6723-6726.
- [16] Shkuratov Y, Muinonen K, Bowell E, Peltoniemi J, Kreslavsky M, Stankevich D, Tishkovetz V, Opanasenko N, Melkumova L, A critical review of theoretical models for the negative polarization

- of light scattered by atmosphereless solar system bodies, *The Earth, Moon, and Planets* 1994; 65:201.
- [17] Shkuratov Y, On the origin of the opposition effect and negative polarization for cosmic bodies with solid surface, *Astronomical Circular (Sternberg State Astron Inst, Moscow)* 1985; 1400:3–6.
- [18] Mishchenko M, Luck JM, Nieuwenhuizen T, Full angular profile of the coherent polarization opposition effect, *Journal of Optical Society of America A* 2000; 17:888–891.
- [19] Shkuratov Y, Ovcharenko A, Zubko E, Miloslavskaya O, Muinonen K, Piironen J, Nelson R, Smythe W, Rosenbush V, Helfenstein P, The Opposition Effect and Negative Polarization of Structural Analogs for Planetary Regoliths, *Icarus* 2002; 159:396–416 .
- [20] Mishchenko M, Dlugach J, Liu L, Rosenbush V, Kiselev N, Shkuratov Y, Direct solutions of the Maxwell equations explain opposition phenomena observed for high-albedo solar system objects, *Astrophysical Journal Letters* 2009; 705:L118.
- [21] Nelson RM, Boryta MD, Hapke BW, Manatt KS, Shkuratov Y, Psarev V, Vandervoort K, Kroner D, Nebedum A, Vides CL, Quinones J, Laboratory simulations of planetary surfaces: Understanding regolith physical properties from remote photopolarimetric observations, *Icarus* 2018; 302:483-498.
- [22] Stankevich D, Shkuratov Y, Muinonen K, Shadow-hiding effect in inhomogeneous layered particulate media, *Journal of Quantitative Spectroscopy and Radiative Transfer* 1999; 63:445-458.
- [23] Stankevich D, Shkuratov Y, Grynko Y, Muinonen K, Computer simulations for multiple scattering of light rays in systems of opaque particles, *Journal of Quantitative Spectroscopy and Radiative Transfer* 2003; 76:1-16.
- [24] Stankevich D, Shkuratov Y, Monte Carlo ray-tracing simulation of light scattering in particulate media with optically contrast structure, *Journal of Quantitative Spectroscopy and Radiative Transfer* 2004; 87:289-296.
- [25] Shkuratov Y, Grynko Y, Light scattering by media composed of semitransparent particles of different shapes in ray optics approximation: consequences for spectroscopy, photometry, and polarimetry of planetary regoliths, *Icarus* 2005; 173:16-28.
- [26] Grynko Y, Shkuratov Y, Videen G, Polarization of near-forward-scattered light from particulate substrates illuminated at near-grazing angles, *Journal of Quantitative Spectroscopy and Radiative Transfer* 2006; 101: 522-526.
- [27] Grynko Y, Shkuratov Y, Ray tracing simulation of light scattering by spherical clusters consisting of particles with different shapes, *Journal of Quantitative Spectroscopy and Radiative Transfer* 2007; 106:56-62.
- [28] Grynko Y, Shkuratov Y, Light scattering from particulate surfaces in geometrical optics approximation. In: *Light scattering reviews*, vol. III, A. Kokhanovsky, ed. (Springer, Berlin, 2008) pp. 329– 382.
- [29] Schröder SE, Grynko A, Pommerol A, Keller HU, Thomas N, Roush TL, Laboratory observations and simulations of phase reddening, *Icarus* 2014; 239:201-216.

- [30] Väisänen T, Martikainen J, Muinonen K, Scattering of light by dense particulate media in the geometric optics regime, *Journal of Quantitative Spectroscopy and Radiative Transfer* 2020; 241:106719.
- [31] Markkanen J, Agarwal J, Väisänen, Penttilä A, Muinonen K, Interpretation of the phase functions measured by the OSIRIS instrument for comet 67P/Churyumov–Gerasimenko, *Astrophysical Journal Letters* 2018; 868:L16.
- [32] Väisänen T, Markkanen J, Hadamcik E, Renard JB, Lasue J, Levasseur-Regourd JC, Blum J, Muinonen K, Scattering of light by a large, densely packed agglomerate of small silica spheres, *Optics Letters* 2020; 45:1679-1682.
- [33] Pattelli L, Egel A, Lemmer U, Wiersma DS, Role of packing density and spatial correlations in strongly scattering 3D systems, *Optica* 2018; 5:1037-1045.
- [34] Egel A, Pattelli L, Mazzamuto G, Wiersma DS, Lemmer U, CELES: CUDA-accelerated simulation of electromagnetic scattering by large ensembles of spheres, *Journal of Quantitative Spectroscopy and Radiative Transfer* 2017; 199:103–110.
- [35] Pitman KM, Kolokolova L, Verbiscer AJ, Mackowski DW, Joseph ECS, Coherent backscattering effect in spectra of icy satellites and its modeling using multi-sphere T-matrix (MSTM) code for layers of particles, *Planetary and Space Science* 2017;149:23-31.
- [36] Bertrand M, Devilez A, Hugonin JP, Lalanne P, Vynck K, Global polarizability matrix method for efficient modeling of light scattering by dense ensembles of non-spherical particles in stratified media, *Journal of the Optical Society of America A* 2020; 37:70-83.
- [37] Hesthaven JS, Warburton T, Nodal High-Order Methods on Unstructured Grids: I. Time-Domain Solution of Maxwell's Equations, *Journal of Computational Physics* 2002; 186:186-221.
- [38] Grynko Y, Shkuratov Y, The scattering matrix of transparent particles of random shape in the geometrical optics approximation, *Optics and Spectroscopy* 2002; 93:885-893.
- [39] Grynko Y, Shkuratov Y, Scattering matrix calculated in geometric optics approximation for semitransparent particles faceted with various shapes, *Journal of Quantitative Spectroscopy and Radiative Transfer* 2003; 78:319-340.
- [40] <https://pybullet.org>
- [41] Zhai PW, Lee YK, Kattawar GW, Yang P, Implementing the near-to-far-field transformation in the finite-difference time- domain method, *Applied Optics* 2004; 43:3738–3746.
- [42] Reichert J, Backes AR, Schubert P, Wilke T, The power of 3D fractal dimensions for comparative shape and structural complexity analyses of irregularly shaped organisms, *Methods in Ecology and Evolution*, 2017; 8:1650-1658.
- [43] Hapke B, Bidirectional reflectance spectroscopy. I. Theory, *Journal of Geophysical Research* 181; 86:3039-3054.
- [44] Shkuratov Y, Starukhina L, Hoffmann H, Arnold G, A model of spectral albedo of particulate surfaces: implication to optical properties of the Moon, *Icarus* 1999; 137:235-246.
- [45] Chandrasekhar S, *Radiative transfer*, Oxford University Press, 1950.

- [46] Van de Hulst, HC Multiple Light Scattering: Tables, Formulas, and Applications, New York: Academic Press, 1980.
- [47] Bondarenko S, Ovcharenko A, Shkuratov Y, Videen G, J. Eversole, M. Hart. Light backscatter by surfaces composed of small spherical particles, *Applied Optics* 2006; 45:3871-3877.
- [48] Shkuratov Y, Bondarenko S, Kaydash V, Videen G, Muñoz O, Volten H, Photometry and polarimetry of particulate surfaces and aerosol particles over a wide range of phase angles, *Journal of Quantitative Spectroscopy and Radiative Transfer* 2007; 106:487–508.